Constraining the timescales of mafic magmatism of the Central Karoo Large Igneous Province using high precision U-Pb zircon geochronology

T. Muedi
AEON-ESSRI (Africa Earth Observatory Network-Earth Stewardship Science Research Institute), Nelson Mandela University, Gqeberha, RSA
Department of Geosciences, Princeton University, Princeton, USA
Council for Geoscience, Pretoria, South Africa
e-mail: tmuedi@geoscience.org.za

S. MacLennan
School of Geosciences, University of the Witwatersrand, Johannesburg, South Africa
Department of Geosciences, Princeton University, Princeton, USA
e-mail: sam7@alumni.princeton.edu; scottangusmac@gmail.com

D. Szymanowski and B. Schoene
Department of Geosciences, Princeton University, Princeton, USA
e-mail: dszymanowski@princeton.edu; bschoene@princeton.edu

J.Ramezani
Earth and Planetary Sciences, Massachusetts Institute of Technology, Cambridge, USA
e-mail: ramezani@mit.edu

J. Oalmann
Earth Observatory of Singapore and Asian School of the Environment, Nanyang Technological University, Singapore
e-mail: joalmann@ntu.edu.sg

B. Linol
AEON-ESSRI (Africa Earth Observatory Network-Earth Stewardship Science Research Institute), Nelson Mandela University, Gqeberha, South Africa
e-mail: bastien.aeon@gmail.com

Abstract

Recent U-Pb high-precision geochronological studies have shown rapid emplacement of the intrusive doleritic component of the Karoo Large Igneous Province (KLIP) in Southern Africa. However, these studies focused on a relatively small geographic and altitudinal region of the KLIP. Additionally, the timing of initiation of extrusive volcanism, preserved in the Drakensberg-Lesotho highlands and its relationship to the intrusive suite, has only been imprecisely constrained by Ar-Ar dates. Here, we present new high-resolution U-Pb zircon ages on dolerite sills and dykes from across the central eastern Karoo Basin (South Africa) at elevations between mean sea level and 1560 m, as well as U-Pb detrital zircon data that can be used to estimate the maximum age of volcaniclastic deposition near the base of the extrusive component of the KLIP. Dolerite samples were taken across two areas: (1) thick dykes exposed along the coast of the Indian Ocean to ~1 600 m flanking the Drakensberg Escarpment in the Eastern Cape; and (2) sills between 20 and 220 m below surface, in a borehole core within the interior of the Karoo Basin, 400 km hinterland from the coastline. Our estimated dolerite emplacement ages span a range of *ca.* 80 thousand years (Kyr), between 183.122 ± 0.029/-0.061 and 183.042 ± 0.042/-0.072 million years ago (Ma), and fall within the 331 +60/-54 Kyr age range previously established for magmatism related to the KLIP, despite the marked increase in sampling coverage in terms of area and altitude in this study. Therefore, KLIP geochronology is consistent with other LIPS such as the Siberian and Deccan Traps that supports the hypothesis of rapid emplacement timescales (<1 Myr). Additionally, these data are consistent with, but better delineate that the KLIP in southern Africa appears to be *ca.* 500 Kyr older than the main phase of magmatism in the Ferrar LIP of Antarctica. Detrital zircons from the basal volcanic sequence of the Drakensberg Group exhibit age peaks at *ca.* 1 and 0.5 Ga, typical of the surrounding Namaqua-Natal and Pan-African basement rocks, as well as younger peaks at *ca.* 260 and 200 Ma that likely relate to source provenances from south-western Gondwana and reworking of the Karoo Supergroup sedimentary rocks. High-precision U-Pb dates of the youngest zircon grains result in a maximum depositional age for the basal pyroclastics of 185.25 ± 0.25 Ma, allowing for a *ca.* 2 Myr offset with the intrusive Karoo dolerite suite.

Introduction

Lowermost Jurassic dolerites, outcropping throughout much of Southern Africa and covering an area of more than half a million square kilometers, preserved as dykes, sills and basalts are referred to as the Karoo Large Igneous Province (KLIP). This large magmatic province has been linked to the early stages of separation between East and West Gondwana (du Toit. 1937, Reeves et al., 2016, Mueller and Jokat. 2019, Peace et al., 2019) and has been associated with rock sequences of the Donning Maud Land region of East Antarctica, known as the Ferrar dolerites that define the Ferrar Large Igneous Province (Riley et al., 2005, Riley et al., 2006, Heinonen et al., 2010, Elliot, et al., 1999, Burgess et al., 2015, Craddock et al., 2017; Luttinen 2018) (Figure 1A). Since these two separate regions preserve large extractions of mantle-derived basaltic magma and were likely associated with high levels of CO_2 and SO_2 outgassing during early Gondwana break-up (Sensarma et al., 2018), establishing their potential temporal links to ecological and climatic disturbances such as the Pliensbachian-Toarcian boundary (*ca.* 183.5 Ma; Ruhl et al., 2016) and the Toarcian Oceanic Anoxic Event (T-OAE; *ca.* 183.25 Ma; Sell et al., 2014), as recorded in both marine and continental settings (e.g. Burgess et al., 2015, Slater et al., 2019, De Lena et al., 2019) is essential. The available geochronology suggests that the T-OAE is related to KLIP magmatism (Pittet et al., 2014, Corfu et al., 2016, Them et al., 2018, Greber et al., 2020). However, earlier biogeochemical disturbances marking the late Pliensbachian previously correlated with the KLIP, but now more precisely dated at circa 186.74 ± 0.06 to 185.94 ± 0.39 Ma, precede the KLIP by *ca.* 2 Myr, precluding a causal link (De Lena et al., 2019).

The Matatiele area of the Eastern Cape Province of South Africa, flanking the Drakensberg-Lesotho Mountains, exhibits well-exposed dolerites dykes and sills up to elevations above 3 000 m (Figure 1). Here, field observations and geochemistry suggest a link between emplacement of the Karoo dolerites and Drakensberg Group lavas (du Toit. 1911a, and 1954, Eales and Marsh 1979, Bristow 1980, Bristow and Saggerson 1983, Rollinson 1993, Marsh et al., 1997, Mitha, 2006, Muedi, 2019). However, their relationship remains equivocal due to ambiguous field evidence and imprecise geochronological data. $^{40}Ar/^{39}Ar$ dating on lavas yielded eruption ages between 189 and 178 Ma (e.g. Duncan et al., 1997, Jourdan et al., 2004, 2005, 2007, Moulin et al., 2011, 2017) and U-Pb analyses on zircons from dolerites across large areas of the Karoo yielded ages between *ca.* 181 and 184 Ma (Svensen et al., 2012). High-precision Isotope Dilution Thermal Ionization Mass Spectrometer (ID-TIMS) U-Pb geochronology of Sell et al., 2014, Burgess et al., 2015 and Greber et al., 2020 constrain a short duration of Karoo dolerite dyke and sill magmatism on the scale of a few hundred thousand years at *ca.* 183 Ma. However, the spatial distribution of the dated samples in these three previous studies is limited to the relatively high elevation area (~1 000 m) east of the Drakensberg Mountains (see Figure 1).

Here we present new high-resolution ID-TIMS U-Pb dates on selected zircons from dolerite samples collected along a transect between the eastern South African coast and the Drakensberg Mountains to the west, as well as from a drill core located 400 km away, in the central Karoo Basin, in order to test for potential age variations related to location, elevation or direction and rate of magma propagation (Figure 1A). In addition, we also present Laser Ablation Inductively Coupled Mass Spectrometry (LA-ICPMS) zircon U-Pb dates on two samples from volcaniclastic tuffs, as well as higher precision ID-TIMS U-Pb dates on their youngest grains, in order to constrain the maximum depositional age of volcanics at the base of the KLIP.

Geological setting of the Karoo dolerite suite

The Karoo dolerite sills analyzed in this study were sampled across central and eastern South Africa, covering an area of approximately 1 000 km² where they intrude into the Triassic strata of the Beaufort Group (Figure 1). Dykes linked to these sills also intrude mafic volcanics of the overlying Lower Jurassic Drakensberg Group (du Toit, 1920; Bristow and Saggerson, 1983; Ivanov et al., 2017; Coetzee and Kisters., 2018), which forms the upper sequences of the Karoo Supergroup (du Toit 1954; Johnson et al., 2006; Linol and de Wit, 2016; Figures 1

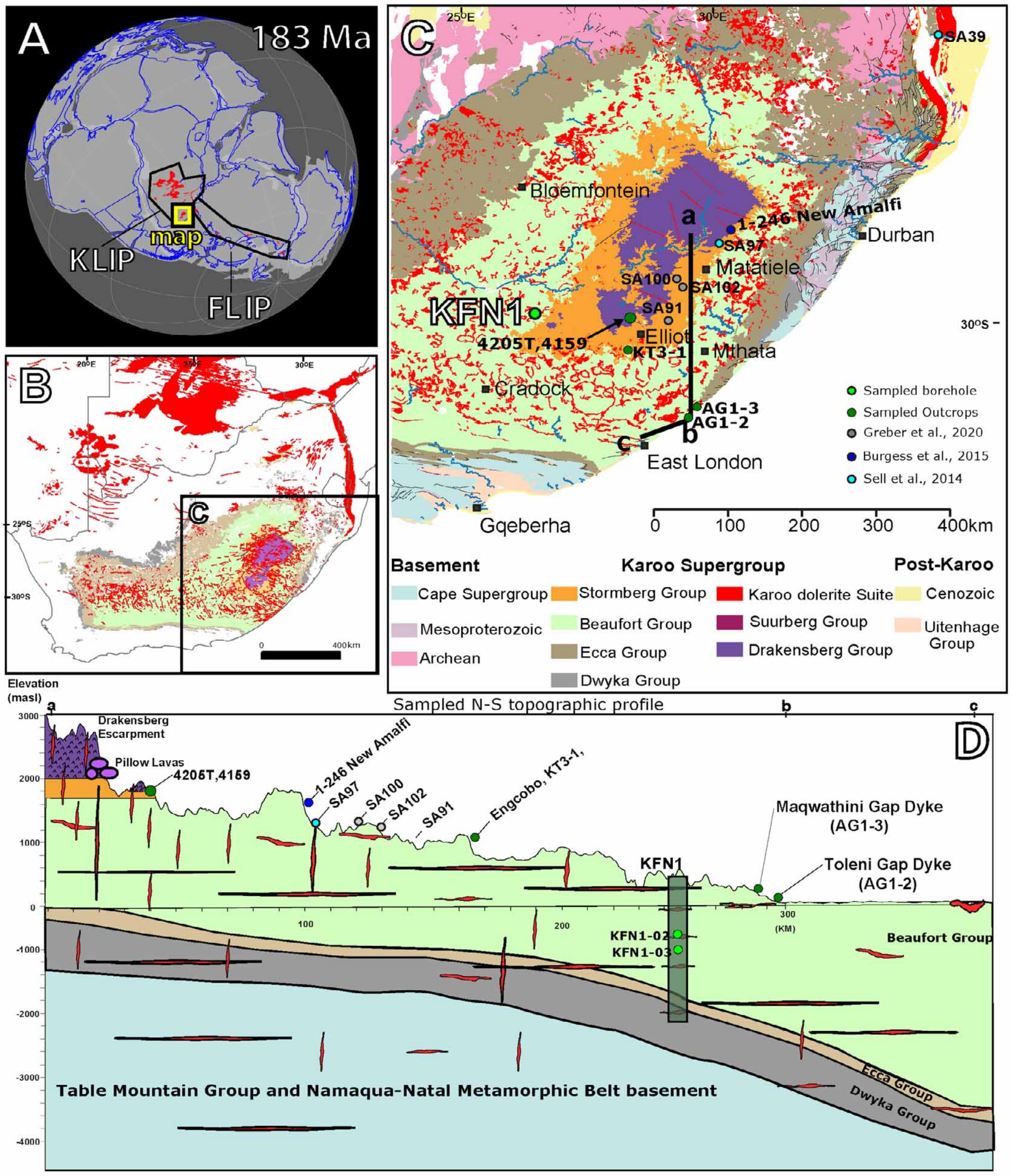

Figure 1. *(**A**) Location of the Karoo Large Igneous Province (KLIP) in its reconstructed Gondwana position at 183 Ma, linked to the similar aged Ferrar Large Igneous Province in Antarctica (Boyden et al., 2011). (**B**) Geological map showing Karoo igneous rocks across southern Africa in red. The black square indicates the location of the detailed geological map shown in 1C. (**C**) Geological map of the study area and the location of an north-south orientated cross-section (a-b-c) highlighting dolerite sample locations from deep below sea-level up to 1800 masl, flanking the southern Drakensberg Group volcanics. The sample locations for this current study and those from previous investigations of Sell et al., 2014), Burgess et al., 2015) and Greber et al., 2020 are shown (**D**) Geological cross-section (a-b-c) from the Lesotho highlands to the southern African coast, showing the main lithological units and geochronologic sample locations. Green (KFN1) is a drill core, lime dots represent collected borehole samples, grey, blue and cyan symbols represent the sample locations from Greber et al., 2020, Burgess et al., 2015 and Sell et al., 2014, respectively.*

and 2). The Clarens Formation (100 to 300 m thick), formerly known as Cave sandstones (du Toit, 1954) is stratigraphically below the mafic volcanics. This marker unit consists of yellow-white fine- to medium-grained sandstones and mudstones, interpreted to be deposited in desert-like paleo-environments and is capped by volcanics that may terminate the Karoo Supergroup (du Toit, 1911b; Coetzee and Kisters., 2018; Bordy et al., 2020). The lowermost volcanic rocks of the Drakensberg Group in the studied area outcrop at 1720 to 1750 m, and the contact with underlying sandstones is erosive (du Toit, 1954; Eales and Marsh, 1979; Duncan et al., 1997; Moulin et al., 2016). In places, the basaltic sequences preserve 20 to 50 m thick pillow lavas and variable thicknesses >100 to 300 m of mafic tuffs (Lock et al., 1974; de Wit et al., 2020). In certain cases, 2 to 10 m thick vertical dolerite dykes traverse westwards from the coastal region across the entire volcanic stratigraphy (see Figure 1B for prefered dyke orientations), implying that dolerite magmatism continued throughout the eruption of mafic volcanics of the Drakensberg Group.

Samples

Samples of dolerite that covers a large area and at various elevations between 0 and 1600 m were collected. Two dolerite dykes (AG1-2 and AG1-3), each approximately 200 m thick and sub-vertical, often referred to as the "Gap dykes" (Moore and Moore, 1965) were sampled northeast of East London (Figure 1). These dykes trend parallel 10 km from each other and perpendicular to the east coast (Walker, 1943; Moore, 1965; Neumann et al., 2020). These dolerites can be traced continuously for about 300 km inland and are also inferred to be present in the subsurface from geophysics and drill cores. They mainly consist of plagioclase feldspar, pyroxene, with minor biotite and amphibole. Zircons separated from these two samples are euhedral and brownish to colorless. They are elongated with 150 to 300 µm length and 50 to 100 µm width. Some zircons are truncated and fractured, likely due to the crushing process.

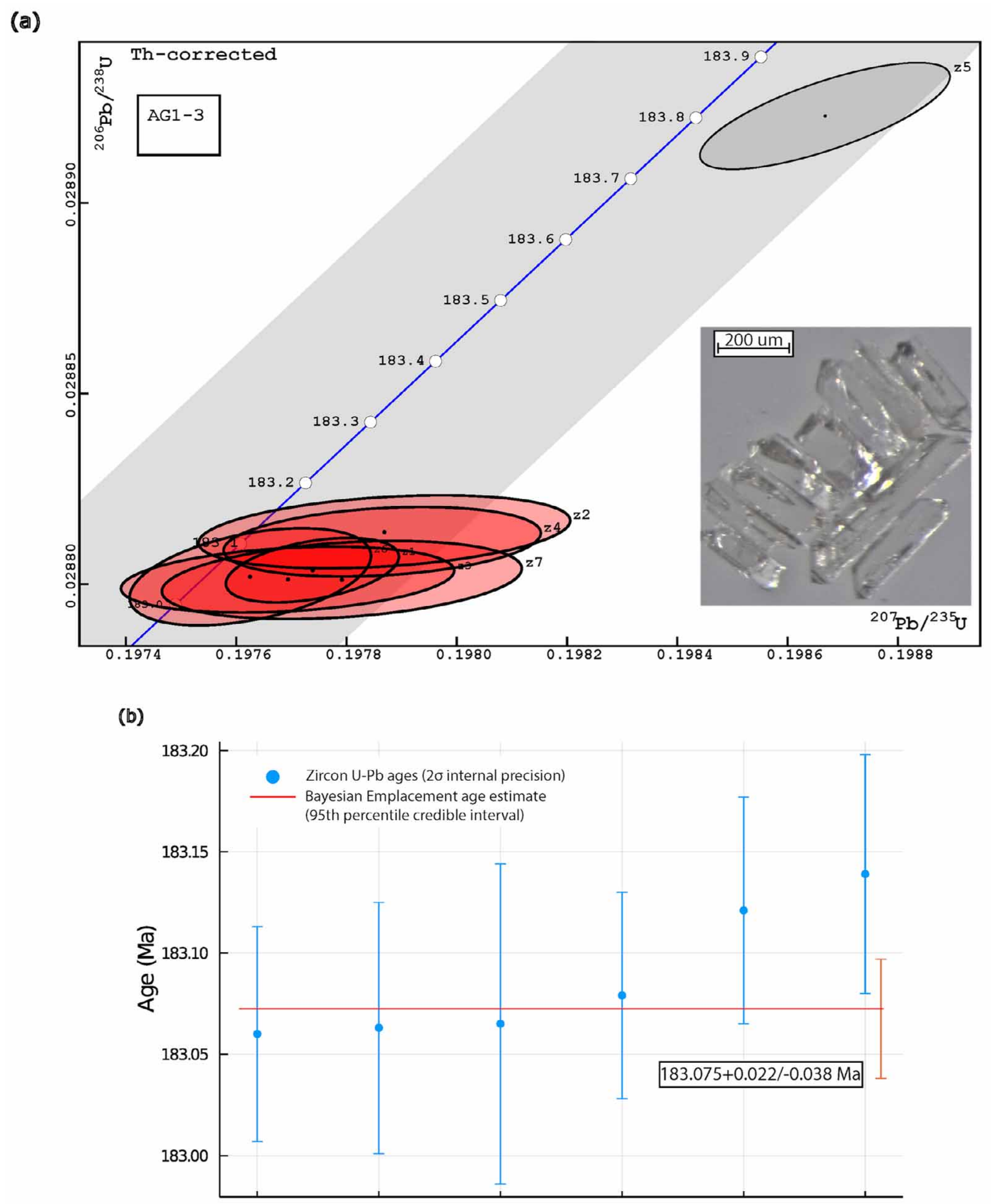

Figure 2. AG1-3 U-Pb results. (a) Conventional concordia diagram and photomicrograph of the analysed zircons; analyses in grey are excluded from emplacement age calculations. The shaded band is the concordia error envelope arising from uncertainty in U decay constants. (b) Rank order $^{206}Pb/^{238}U$ date plot (2σ analytical uncertainty) showing the resulting Bayesian emplacement age estimate and 95th percentile limits of the distribution.

Two dolerite sill samples (KFN1-02 and KFN1-03) were collected for U-Pb zircon analysis from the drill core on Klipfontein Farm (drilled in the 1960s) at a depth of *ca.* 1 000 and 1 200 m. The extracted zircons exhibit various crystal shapes and sizes (Figure 5a) but are generally prismatic and frequently fractured, mostly smoky brownish-black to colorless and 100 to 300 µm long with widths of approximately 80 to 100 µm.

An additional outcrop dolerite sample (KT3-1) was collected in the Matatiele area near the town of Ngcobo at 1 560 m (Figure 1). Sample KT3-1 is from near the base of a medium to coarse grained dolerite sill, 383 m thick. It is emplaced at the highest level of the Beaufort Group sedimentary rock sequences, but below and separated from the southern volcanics of the Drakensberg Group. The dolerite comprises plagioclase, olivine, pyroxene and minor biotite.

Two rock samples of fine-grained siliciclastics or tuffite that overlie volcanic breccia near the base of the Drakensberg Group (see Figure 1) were sampled for detrital zircon geochronology. Sample 4159 is located below the lowermost basaltic lava in the Loch Bridge section (see de Wit et al., 2020). This sample is a grey, laminated very fine sandstone that overlies matrix-supported volcaniclastic breccia. Sample 4205T was taken from slightly higher up in the stratigraphy and is a blue fine-grained sandstone that overlies andesitic breccia in the Bellmore section (Lock et al., 1974).

Analytical methods

The samples, each about 2 to 5 kg, were carefully split, crushed, milled and sieved. The fine-grained, low-density (feldspathic) material was removed by hand-washing in water. The heavy minerals were further concentrated via magnetic and density separation methods using a Frantz magnetic separator and high-density liquids at the MIT Isotope Lab in USA and at the AEON Earth minilab of Nelson Mandela University, Geoscience department at the University of Witwatersrand and at the Council for Geosciences in South Africa. Two coarse-grained granophyric dolerite samples (AG1-2, AG1-3) and three coarse grained dolerites (KT3-1, KFN01-02 and KFN01-03) yielded enough zircon grains for U-Pb geochronology. U-Pb isotopic analyses were performed at TIMS facilities at MIT and Princeton University. AG1-3 and KT3-1 were analyzed at MIT, while AG1-2, KFN1-02 and KFN1-03 were analyzed at Princeton University. Both laboratories use the same isotopic tracer solution ^{202}Pb-^{205}Pb-^{233}U-^{235}U (ET2535) and data reduction procedure, meaning that the U-Pb dates obtained at MIT or Princeton University are directly comparable.

Between 5 and 15 zircons per sample were handpicked under a binocular microscope based on crystal morphology and clarity (detailed sample preparation procedures are available in Muedi, (2019) and were thermally annealed at 900°C for 60 hours in a muffle furnace. Individual zircon grains were placed in Teflon capsules and leached in concentrated hydrofluoric acid (HF) at either 190°C or 210°C for 12 hours (aliquots are labelled indicating which temperature they were chemically abraded at). At MIT, the higher chemical abrasion temperature of 210°C was used for all analyses. At Princeton, the lower chemical abrasion temperature of 190°C was initially used. However, chemical abrasion temperatures were subsequently increased in an attempt to eradicate residual Pb loss. Following chemical abrasion, the residual zircon grains were rinsed a number of times in dilute nitric acid, 6N hydrochloric acid (HCl) and milliQ water. After rinsing, the zircon grains were spiked with the EARTHTIME ^{202}Pb-^{205}Pb-^{233}U-^{235}U (ET2535) tracer solution (see McLean et al., 2015 for details) and dissolved in concentrated HF for 48 hours at 210°C. Following dissolution, the solutions were dried and redissolved in 6N HCl overnight in preparation for ion chromatography. Uranium and Pb were purified by an HCl-based column chemistry using AG-1 X8 200 to 400 mesh anion-exchange resin following a procedure modified from Krogh (1973). For more thorough descriptions of the analytical methods used at Princeton University and MIT, see Schoene et al., 2019 and Ramezani et al., 2011, respectively. All reported ages are corrected for initial Th disequilibria unless otherwise stated. Details regarding how the correction for initial Th disequilibrium are available in the data supplement. (Supplementary data files are archived in the South African Journal of Geology repository (https://doi.org/10.25131/sajg.125.0009.sup-mat))

Emplacement ages were estimated using a Bayesian Markov Chain Monte Carlo technique; see Keller et al., 2018, Schoene et al., 2019 and Kinney et al., 2021 for further details regarding this methodology. Given that the zircons dated in this study are from coarse-grained mafic sills and dykes, zircon saturation is expected to only occur at very high crystallinities, where small pockets of melt enriched in incompatible elements remain. For this reason, the prior used for all Bayesian analysis was a half-normal distribution in order to approximate the increase in zircon saturation expected during and directly after emplacement. In order to make comparisons with the previous high-precision U-Pb zircon studies, we reanalyzed the geochronological data of Sell et al., 2014, Burgess et al., 2015 and Greber et al., 2020 using the same Bayesian scheme and the same zircon selection criteria. These newly interpreted ages are shown in Table 1.

In the case of the detrital zircon samples 4205T and 4159, zircon grains were picked and placed onto double sided tape, where epoxy was poured onto them to create mounts. Laser ablation inductively coupled plasma mass spectrometry (LA-ICP-MS) U-Pb analysis was carried out at the Earth Observatory of Singapore, Nanyang Technological University using a Teledyne/Photon Machines Analyte G2 193 nm excimer laser ablation system coupled to a Thermo-Fisher-Scientific Element 2 sector field ICP-MS. Sample standard bracketing was implemented using zircon reference materials for calibration and quality control, and data were reduced using Iolite v. 4.4.5 (Paton et al., 2011). Details of the analytical parameters including the results from secondary reference materials can be found in Appendix B in the supplementary data.

The youngest and most euhedral grains from sample 4205T were extracted out of the epoxy mounts and analysed at Princeton University using the same ID-TIMS methods described above. The objective was to try and place a precise maximum depositional age on the base of the volcanics of the Drakensberg Group.

Table 1. Summary of the ID-TIMS U-Pb Bayesian statistics geochronology dates of the Karoo Basin, South Africa. See supplementary data for details.

Latitude	Longitude	Elevation (masl)	Estimated emplacement age (Ma)	95% credible interval limits		Host rock	Mineral	Sample Number
-30.252417	29.1139	1617	182.93	+0.133	-0.284	Sandstone, (Tarkastad Subgroup)	Baddeleyite and zircons	SA97, Sell et al., 2014
-29.1547	30.2444	1580	183.234	+0.03	-0.053	Sandstone, (Tarkastad Subgroup)	Zircons	1-247, Burgess et al., 2015
-31.0782	28.350200	1272	182.902	+0.085	-0.12		Zircons	SA91, SA100, SA102, Greber et al., 2020
-27.99153	31.6189	1350	183.042	+0.042	-0.072	Sandstone (Tarkastad Subgroup)	Zircons	KT3-1, Ngcobo, this study
-30.5592	25.3077	223	183.122	+0.029	-0.061	Sandstone (Adelaide Subgroup)	Zircons	KFN1-02, KFN-03 borehole Klipfontein, this study
-30.8669	29.6858	3	183.075	+0.022	-0.038	Sandstone (Adelaide Subgroup)	Zircons	AG1-3, Maqwathini, this study

Geochronological results

The U-Pb zircon results are described below and summarized in Table 1. All uncertainties are presented as 95th percentile credible interval unless otherwise stated.

Gap Dyke dolerite at Maqwathini (AG1-3)

Ten zircons were extracted from this dolerite dyke sample and seven zircons were analyzed for their U-Pb isotopic composition (Figure 2). Six of these zircons yielded concordant U-Pb dates of *ca.* 183 Ma. One analysis is significantly older at *ca.* 183.7 Ma, possibly due to inheritance of an older zircon core from the host rocks. Using Th-corrected ages for six overlapping zircons in the Bayesian scheme (Z1, Z2, Z3, Z4, Z6, and Z7) yields an emplacement age estimate at *ca.* 183.075 + 0.022/-0.038 Ma (Figure 2).

Ngcobo dolerite sill (KT3-1)

Four zircons (Z2, Z3, Z4 and Z5) free from crystallographic imperfections and inclusions were selected for U-Pb analysis. Three of the analyzed zircons exhibit very similar U-Pb dates of *ca.* 183.1 Ma, while a fourth (Z5) is slightly older at *ca.* 183.25 Ma. Using all four grains for the Bayesian inference results in a median age of *ca.* 183.042 +0.042/-0.072 Ma (Figure 3).

Gap dyke dolerite at Toleni (AG1-2)

Ten zircon grains were analyzed from sample AG1-2 (Figure 4). There is significant dispersion in the zircon U-Pb data, yielding very few overlapping dates, varying between *ca.* 181 and 189 Ma. This heterogeneity suggests either significant residual Pb loss, local contamination with xenocrystic zircon cores during emplacement and/or a more diverse history of KLIP magmatism recorded by magmatic zircon (Figure 4). Three zircons dates (Z4, Z5, and Z9) overlap within uncertainty and may represent the true emplacement age of this dyke. However, due to the complicated age dispersion we choose not to assign an emplacement age to this sample.

Kransfontein dolerite sill in borehole core (KFN1-02)

In total, 26 zircon grains were extracted and processed for U-Pb isotope analysis (Figure 5a). A number of zircons were either lost during transfer to Teflon vials or were completely dissolved during chemical abrasion, as reflected by the absence of any radiogenic Pb in the analyzed aliquots. The first 17 grains that were analyzed showed complicated date dispersion patterns, in a similar fashion to AG1-2. These zircons range in age between *ca.* 184 to 181.6 Ma with a cluster of dates around *ca.* 183.17 Ma and were chemically abraded at a temperature of 195°C. In order to determine whether the cluster of overlapping dates was an accurate estimate of emplacement age or the result of residual Pb loss, a further nine zircons were selected (Z1s to Z9s) to undergo chemical abrasion at a higher temperature of 210°C in an attempt to mitigate any residual Pb loss. These analyses also show significant age variation, possibly implying continued survival of metamict zircon despite higher chemical abrasion temperatures, the presence of inherited zircon cores or protracted zircon saturation in mafic magmas. However, several of the grains that were chemically abraded at higher temperatures overlap with the cluster of grains at *ca.* 183.15 Ma, implying that this cluster is a reasonable estimate of the emplacement age. Using the zircons from this age cluster to constrain the timing of emplacement using Bayesian inference results in a median age of *ca.* 183.122 +0.029/-0.061 Ma (Figure 6b and c). The Th/U of the all of the analyzed zircons is relatively consistent at *ca.* 3.5 and shows no relationship with age, further supporting the

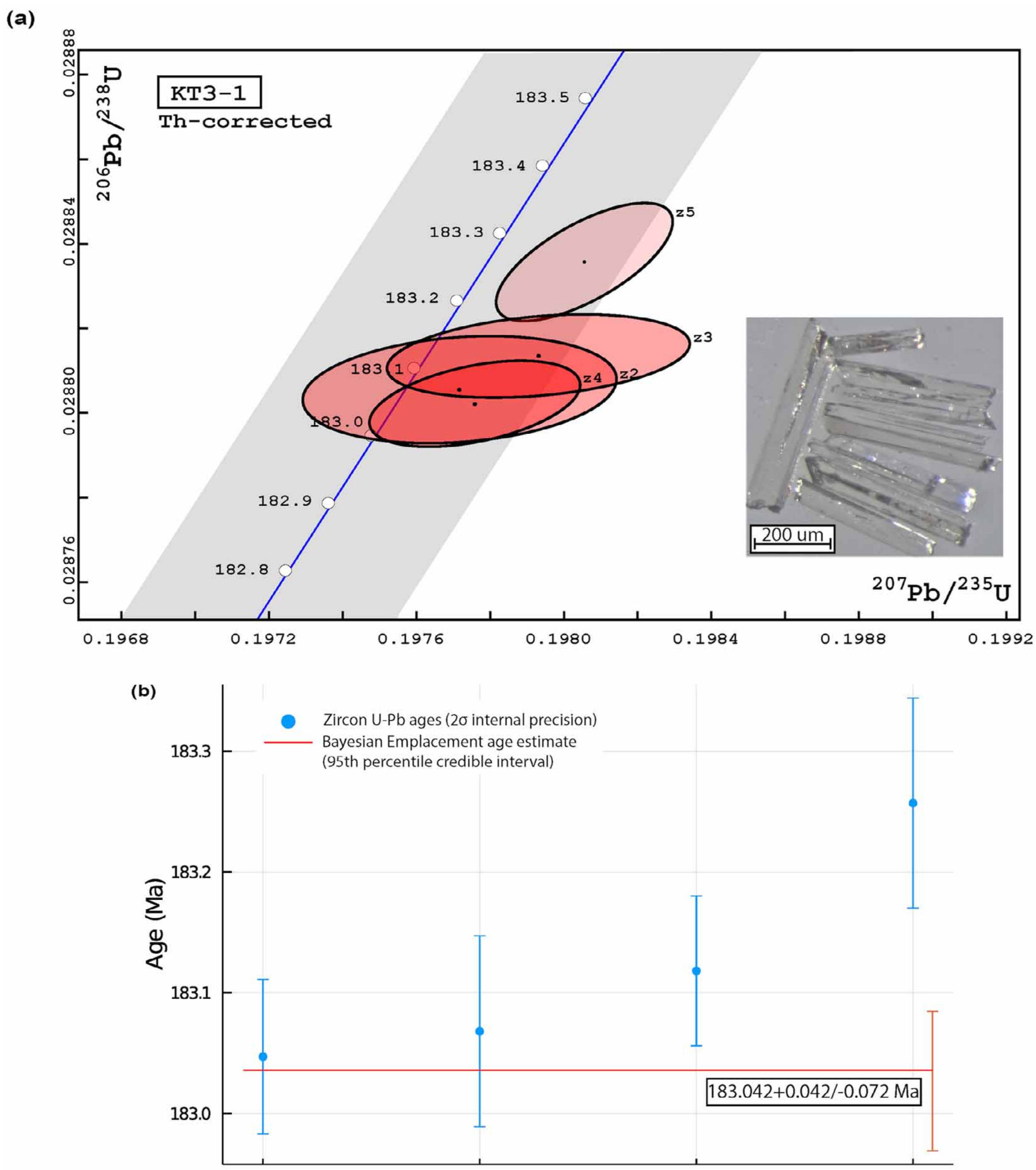

Figure 3. ***(a)*** *KT3-1, conventional concordia diagram and photomicrograph of the analyzed zircons; analyses in grey are excluded from age calculation. Shaded band is the concordia error envelope arising from uncertainty in U decay constants.* ***(b)*** *Rank order* $^{206}Pb/^{238}U$ *date plot (2σ analytical uncertainty) showing the resulting Bayesian emplacement age estimate and 95th percentile limits of the distribution.*

interpretation that the excess age dispersion may be the result of residual Pb loss after chemical abrasion.

Kransfontein dolerite sill in borehole core (KFN1-03)

Twenty-one zircons were dated from this core sample. U-Pb dates from the first 12 zircons analyzed span a large range from *ca.* 182.5 to 186 Ma (Figure 6). This variance may be due to a combination of inherited xenocrystic zircon cores, prolonged magmatic growth or residual Pb loss that survived chemical abrasion. In order to eliminate the last possibility, another batch of nine zircons (Z1s to Z9s) were chemically abraded at 210°C for 12 hours. The majority of these zircons completely dissolved during chemical abrasion, but the few grains that did survive chemical abrasion still exhibited relatively large age variations, implying that zircons from this sample record either protracted timescale of magmatic saturation or the inclusion of xenocrystic cores – possibly from the surrounding sedimentary rocks. For these reasons, an emplacement age for this sill has not been estimated.

Lower Drakensberg tuffites 4205T and 4159

For the two detrital zircon samples, 76 and 125 U-Pb analyses were collected for 4205T and 4159, respectively (Figure 7a). Both samples show Namaqua Natal (*ca.* 1 Ga) and Pan African (*ca.* 0.5 Ga) zircon age peaks, as well as significant age peaks centered at *ca.* 200 and 260 Ma. Of the youngest and most euhedral zircon grains from 4205T that were selected for

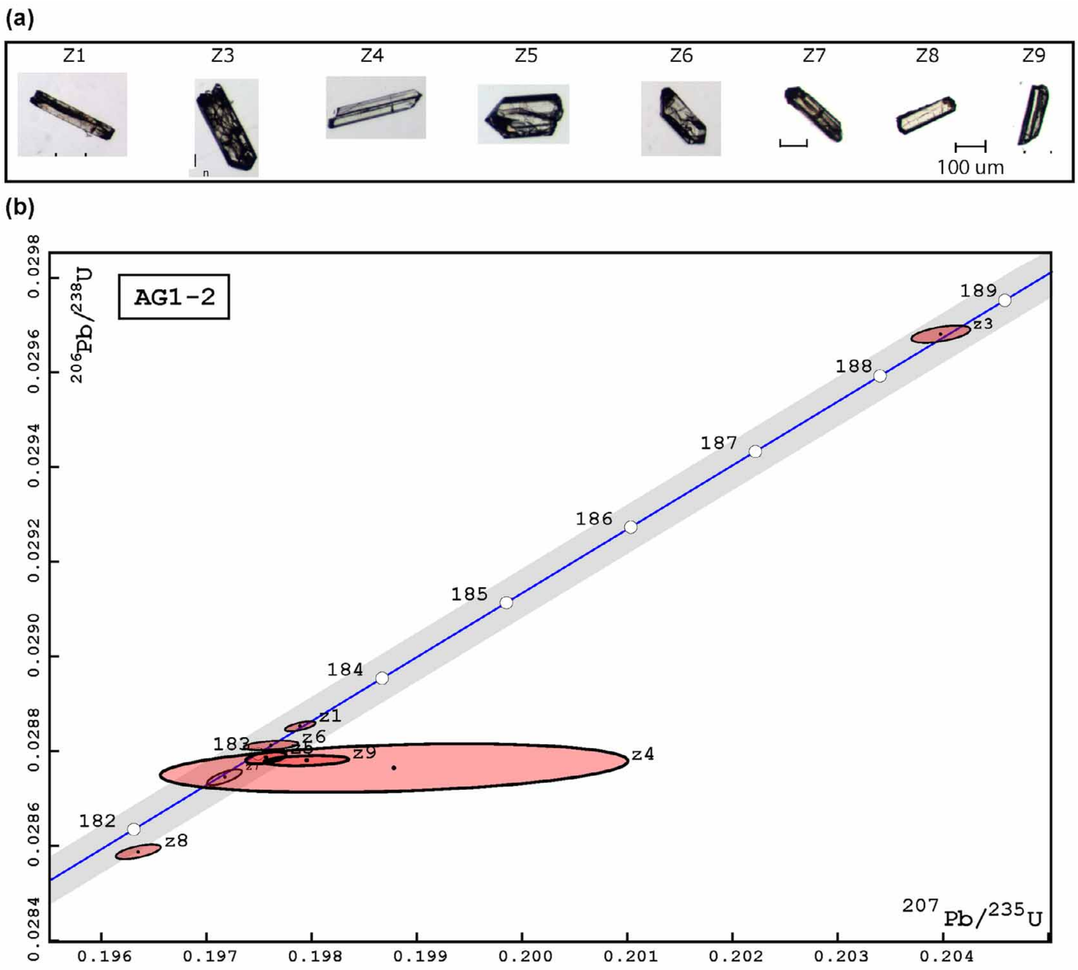

Figure 4. *(**a**) AG1-2 zircons dolerite photomicrographs and (**b**) conventional concordia diagram of the analyzed zircons. The Shaded band is the concordia error envelope arising from uncertainty in U decay constants. Due to the age dispersion in this sample, a Bayesian emplacement estimate was not calculated.*

ID-TIMS analysis, only three survived chemical abrasion. These ages range from *ca.* 187 to 185 Ma, with the youngest grain having an age of *ca.* 185.25 ± 0.25 Ma.

Discussion

Characterizing dolerite age heterogeneity across the Karoo basin LIP

Sample AG1-3 was previously analyzed using ID-TIMS, yielding zircon ages about 0.5 to 1.0 Myrs younger than those in this study, which may be the result of differences in U-Pb spike calibration (e.g. Corfu et al., 2016) and highlights the benefit of using a community-wide U-Pb spike such as EARTHTIME (Condon et al., 2015). In contrast, our new results show significant similarity with the ID-TIMS U-Pb zircon studies of Sell et al., 2014, Burgess et al., 2015 and Greber et al., 2020, which utilize the same isotopic tracer and similar data reduction strategies.

Our dolerite samples span a wide geographic and altitude distribution across the central eastern Karoo Basin. The dolerite sill from Ngcobo (KT3-1) is located at 1 560 m elevation and 100 km away from AG1-3 (Figure 1). Sample KFN01-02 is located about 400 km hinterland. As can be seen on Figure 8, which compiles all available U-Pb zircon dates that use the Earthtime isotopic tracer, KLIP magmatism is constrained to a 330 Kyr time period and shows no resolvable age relationship with altitude or geographic location. These compiled high-resolution U-Pb zircon dates from the KLIP clearly support rapid timescales of magmatism that is effectively synchronous across large parts of the Karoo Basin, supporting the connection between KLIP magmatism and the T-OAE as suggested by Sell et al., 2014; Greber et al., 2020.

Detrital zircons provenances

The two samples of sediment matrix associated with volcanic breccia near the base of the Drakensberg Group show significant Namaqua-Natal (*ca.* 1 Ga) and Pan African (*ca.* 0.5 Ga) age peaks, which can be anticipated given the abundance of these terranes within the Kalahari Shield underlying and surrounding the Karoo Basin. The two oldest dates at *ca.* 2.7 to 2.8 Ga may be locally derived from the Archean Kaapvaal craton.

In contrast, the *ca.* 260 and 200 Ma age peaks coincide with Permian-Triassic continental arc-volcanism along the paleo-Pacific margin of Gondwana, including the 250 to 280 Ma Choiyoi Province (e.g. Kay et al., 1989; Pankhurst et al., 1998; de Wit, 2007; Munizaga et al., 2008; Kleiman and Japas, 2009; Nelson and Cottle, 2019; Morake et al., 2021). Additionally, a magmatism phase at *ca.* 200 Ma- potentially related to initial Gondwana break up- has been identified in Antarctica (Morake et al., 2021), which may have been another source for detrital zircons of this age. These two age peaks have been reported elsewhere in the Karoo, Paraná, and Congo basins (e.g. López-Gamundí, 2006; Fildani et al., 2009; Linol et al., 2015; Canile et al., 2016; Viglietti et al., 2018; Bordy et al., 2020), implying that more likely these young zircons in basal KLIP volcaniclastic sequences represent sediment reworking of some back-arc basin systems. However, the sediment distribution pathways across distances >1 000 km from the southern Gondwanan volcanic belt to the intracratonic basin depositional areas remain poorly resolved, particularly as the opening of the oceans between southern America (Patagonia), Africa, and Antarctica (Peninsula, Ellsworth-Whitmore and East Antarctica) has largely changed the initial paleogeography.

The youngest TIMS analysis of 185.25 ± 0.25 Ma sets for the first time a robust maximum depositional age for basal KLIP

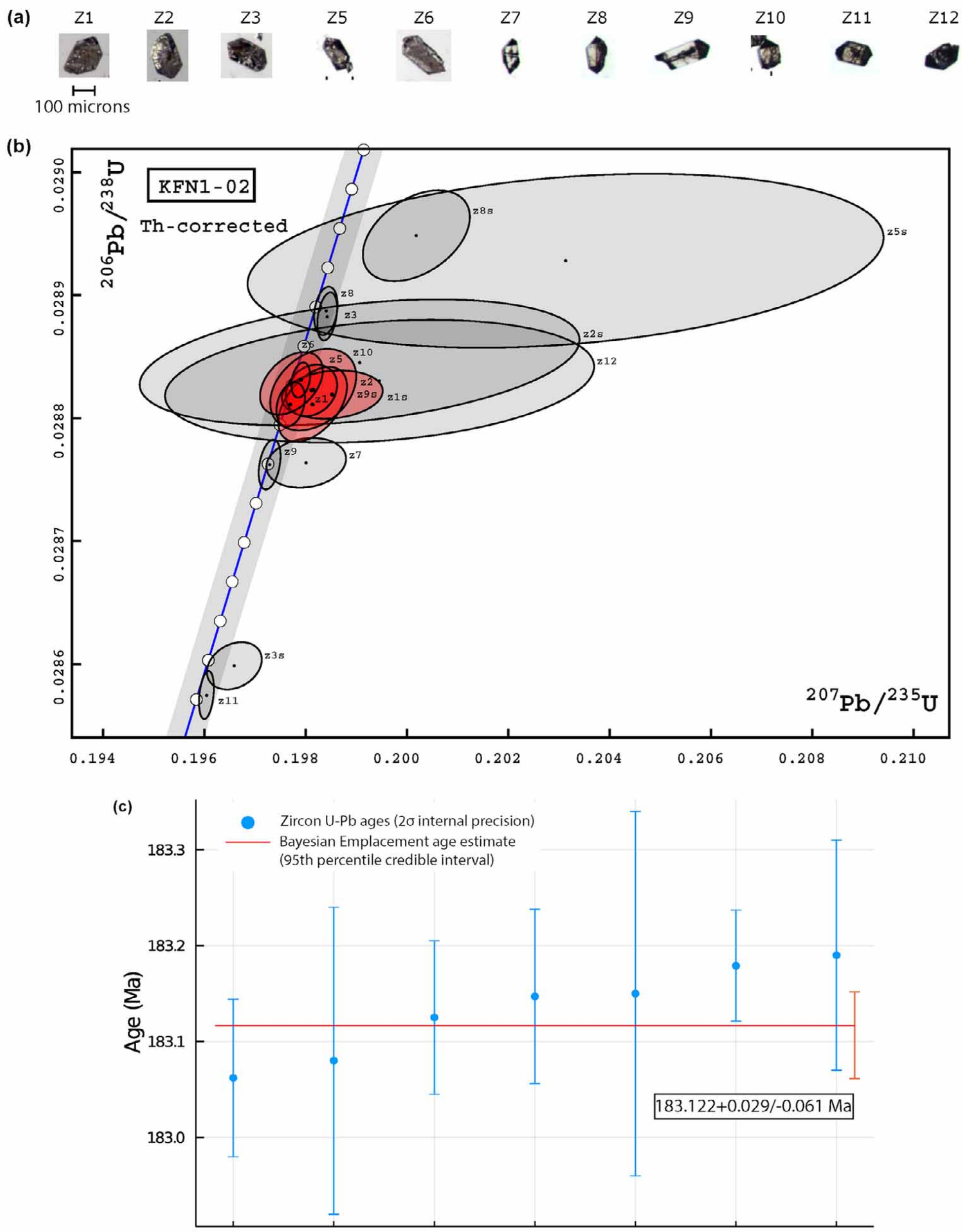

Figure 5. *KFN1-02, (**a**) conventional concordia diagram of analyzed zircons; analyses in grey are excluded from age calculation. Shaded band is the concordia error envelope arising from uncertainty in U decay constants. (**b**) Rank order $^{206}Pb/^{238}U$ date plot (2σ analytical uncertainty) showing the resulting Bayesian emplacement age estimate and 95th percentile limits of the distribution.*

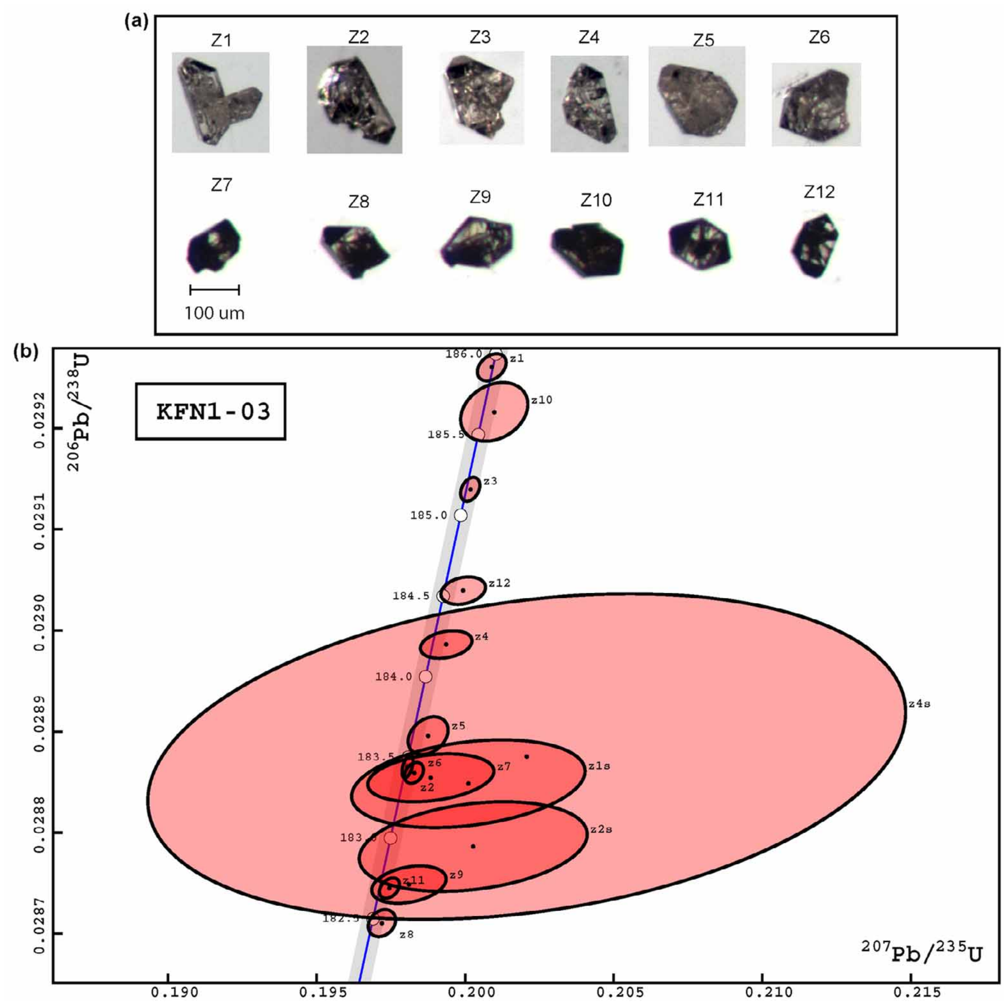

Figure 6. *KFN1-03, (**a**) Photomicrographs of the analyzed zircon grains. (**b**) Conventional concordia diagram showing scattered dates. Grey shaded band is the concordia error envelope arising from uncertainty in U decay constants.*

extrusive volcanism and implies that a *ca.* 2 Myr temporal offset may exist with the intrusive components of the KLIP. High-precision magmatic zircon dates from the basal Drakensberg Group lavas are needed to further elucidate whether this temporal gap truly exists.

Karoo-Ferrar temporal heterogeneity and connections with global carbon cycle perturbations

Figure 9 shows kernel density estimates created using all available high-precision U-Pb zircon dates from the KLIP and FLIP. As mentioned above, the existing KLIP zircon dates from Sell et al., 2014, Burgess et al., 2015 and Greber et al., 2020 were all recomputed using the same Bayesian Markov Chain Monte Carlo technique as was used for our newly presented emplacement age estimates. Zircon grain selection was the same as that used for the weighted mean calculations presented in the publications in each case. The total age distributions for KLIP and FLIP show some overlap but their peak emplacement age probabilities are distinct, with a *ca.* 500 Kyr separation. This data indicates that the KLIP began and ended before the FLIP with only a potential overlap of a few 100's of Kyr, in accordance with previous studies that invoke age differences between the two igneous provinces (e.g. Burgess et al., 2015 and Greber et al., 2020). Our dates also further support temporal correlations of KLIP magmatism to global climate change during the T-OAE, which was temporally constrained at 183.22 ± Ma by Sell et al., 2014. Figure 9 shows a lack of any temporal connection between KLIP intrusive magmatism and late Pliensbachian carbon cycle perturbations as well as the Pliensbachian-Toarcian boundary (in support of previous studies by Sell et al., 2014, De Lena et al., 2019, Greber et al., 2020. However, our maximum depositional age for the base of KLIP extrusive lavas of *ca.* 185.25 Ma, does not rule out the possibility of a temporal link with late Pliensbachian carbon isotope variability, which occurred between *ca.* 186.5 and 184.5 Ma, based on the age model of De Lena et al., 2019. Since large volumes of Karoo lavas erupted below sea level (e.g., Elliot and Fleming, 2008; de Wit et al., 2020), this early phase of the Gondwanan volcanism must have influenced ocean geochemistry but more precise dating of the pillow lavas is needed to test these connections.

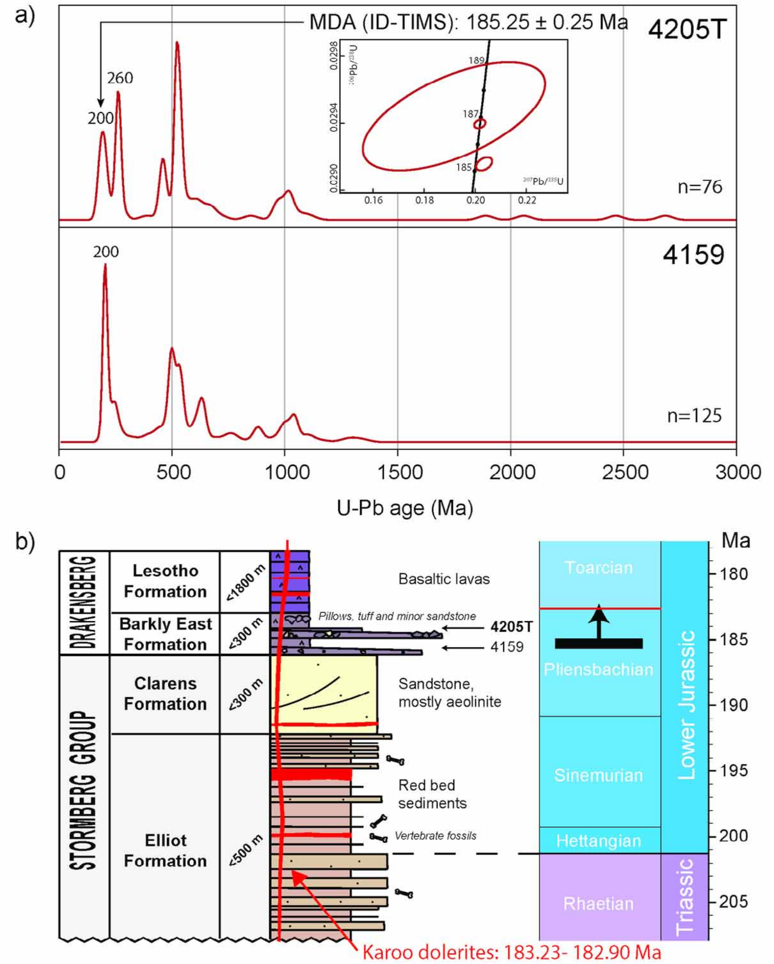

*Figure 7. (**a**) LA-ICP-MS detrital zircon age spectra for volcaniclastic samples 4205T and 4159. The concordia diagram inset shows TIMS U-Pb zircon analyses for three youngest zircons from 4205T. Kibaran, Pan-African and Permian-Triassic detrital zircon age peaks are present. The youngest TIMS zircon analysis of* ca. *185.25 ± 0.25 Ma defines the maximum depositional age for these basal Drakensberg Group volcaniclastic. (**b**) Schematic stratigraphic section of the upper Karoo Supergroup stratigraphy, showing the position of the volcaniclastic rocks sampled for detrital zircon geochronology. The maximum depositional age for the youngest zircons precedes the Pliensbachian-Toarcian boundary by* ca. *2 Myr.*

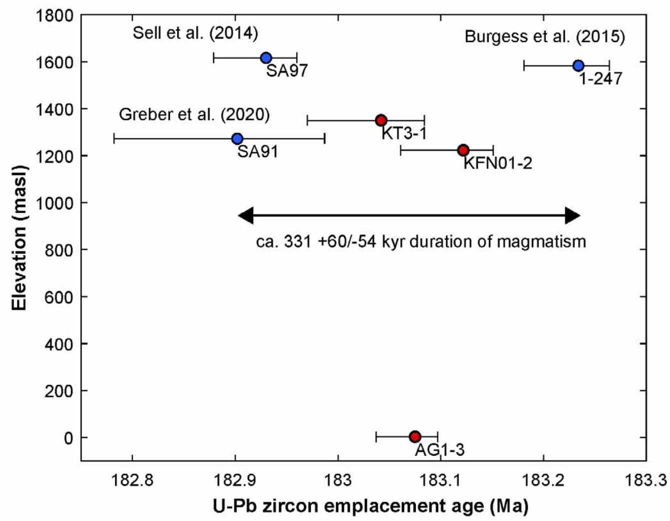

***Figure 8.** Summary of all zircon-based KLIP dolerite emplacement ages using the Earthtime isotopic tracer, from this study and Greber et al., 2020; Burgess et al., 2015; Sell et al., 2014. All emplacement ages are estimated using the same Bayesian approach.*

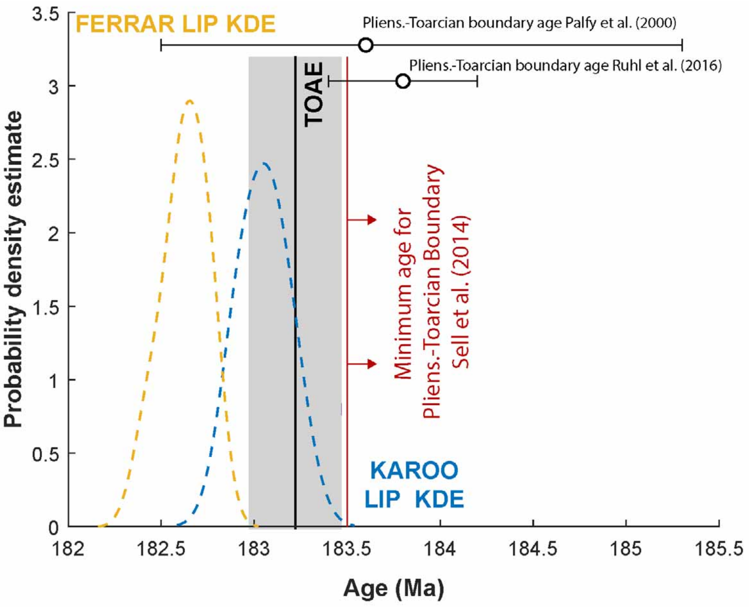

Figure 9. *Kernel Density Estimates for existing high-precision U-Pb ages from the Karoo LIP (Greber et al., 2020; Burgess et al., 2015; Sell et al., 2014 and Ferrar Burgess et al., 2015). The age and two sigma uncertainty for the initiation of the T-OAE are shown in grey (Burgess et al., 2015; Svensen et al., 2017; Greber et al., 2020). Radiometric (Pálfy and Smith, 2000) and cyclostratigraphic (Ruhl et al., 2016) age constraints on the Pliensbachian-Toarcian boundary are shown with black errorbars. A minimum age constraint for the Pliensbachian-Toarcian boundary presented by Sell et al., 2014 is shown in red.*

Conclusions

The currently available (new and compiled) high-precision ID-TIMS U-Pb zircon dates for dolerite sills and dykes of the Karoo large igneous province (KLIP) range from *ca.* 182.9 to 183.25 Ma, resolving a duration of mafic magmatism of <330 Kyr. This timescale is similar to those presented for Large Igneous Provinces across Earth history (e.g. Kasbohm et al., 2021; Park et al., 2020, Schoene et al., 2019). In composite, the available high-precision TIMS ages show no apparent trends between level of emplacement or geographical location in the Karoo Basin and age, implying a regionally synchronous magmatic event. Our new dates on Karoo dolerites combined with previous published ages are older by several hundred thousand years than the Ferrar equivalents flanking Antarctica across a collective triple junction between East (South Africa) and West (Antarctica) Gondwana before the break-up of the supercontinent (Elliot and Fleming, 2000). Lastly, a maximum depositional age of *ca.* 185 Ma for basal KLIP lavas and tuffs leaves the possibility for a significant temporal offset with the intrusive dolerites and highlights the need for high-precision zircon age constraints from the extrusive rocks of the Drakensberg Group to test for a causal relationship with late Pliensbachian climate and carbon cycle perturbations.

Acknowledgements

Maarten de Wit and Samuel Bowring both played critical roles in this study in terms of mentorship and motivation. Unfortunately, Maarten and Sam have both passed away somewhat recently and they are greatly missed by the authors. Their absence is also keenly felt by many in the geoscience community around the world. We would like to thank Grant Cawthorn at the University of Witwatersrand for giving T. Muedi access to the mineral separation lab and also for providing us with the KFN1-02 borehole sample to process. We acknowledge the support from DST-NRF who provided Iphakade funding through the Global Change program. We also thank the Council for Geoscience for their contribution towards the execution of the project, funding and for allowing access to the National Core Library in Donkerhoek and laboratory analysis in Pretoria. This is AEON contribution 204 and Iphakade contribution 274.

References

Bordy, E.M., Abrahams, M., Sharman, G.R., Viglietti, P.A., Benson, R.B.J., Mcphee, B.W., Barrett, P.M., Sciscio, L., Condon, D., Mundil, R., Rademan, Z., Jinnah, Z., Clark, J.M., Suarez, C.A., Chapelle, K.E.J. and Choiniere, J.N., 2020. Earth-Science Reviews A chronostratigraphic framework for the upper Stormberg Group : Implications for the Triassic-Jurassic boundary in southern Africa. Earth-Science Reviews, 203, 103120.

Boyden, J.A., Muller, R.D., Gurnis, M., Torsvik, T.H., Clark, J.A., Turner, M., Ivey-Law, H., Rubin J. and Cannon, J.S., 2011. Next-generation plate-tectonic reconstructions using GPlates. Gplates website, 95-114.

Bristow, J.W. and and Saggerson, E.P., 1983. A general account of Karoo vulcanicity in southern Africa. Geologische Rundschau, 72, 1015-1059.

Burgess, S.D., Bowring, S.A., Fleming, T.H. and Elliot, D.H., 2015. High-precision geochronology links the Ferrar large igneous province with early-Jurassic ocean anoxia and biotic crisis. Earth and Planetary Science Letters, 415, 90-99.

Canile, F.M., Babinski, M. and Rocha-Campos, A.C., 2016. Evolution of the Carboniferous-Early Cretaceous units of Paraná Basin from provenance studies based on U-Pb, Hf and O isotopes from detrital zircons. Gondwana Research, 40, 142-169.

Coetzee, A. and Kisters, A.F.M., 2018. The elusive feeders of the Karoo Large

Igneous province and their structural controls. Tectonophysics, 747-748, 146-162.

Condon, D.J., Schoene, B. and McLean, N.M., Bowring, S.A. and Parrish, R.R., 2015. Metrology and traceability of U-Pb isotope dilution geochronology (EARTHTIME Tracer Calibration Part I). Geochimica et Cosmochimica Acta, 164, 464-480.

Corfu, F., Svensen, H. and Mazzini, A., 2016. Comment to paper: Evaluating the temporal link between the Karoo LIP and climatic-biologic events of the Toarcian Stage with high-precision U-Pb geochronology by Bryan Sell, Maria Ovtcharova, Jean Guex, Annachiara Bartolini, Fred Jourdan, Jorge E. Spangen. Earth and Planetary Science Letters, 434, 349-352.

Cox, K.G., 1992. Karoo igneous activity, and the early stages of the break-up of Gondwanaland. Geological society of london, special publications, 68, 137-148.

Craddock, J.P., Schmitz, M.D., Crowley, J.L., Larocque, J., Pankhurst, R.J., Juda, N., Konstantinou, A. and Storey, B., 2017. Precise U-Pb zircon ages and geochemistry of Jurassic granites, Ellsworth-Whitmore terrane, central Antarctica. Bulletin of the Geological Society of America, 129, 118-136.

De Lena, L.F., Taylor, D., Guex, J., Bartolini, A., Adatte, T., van Acken, D., Spangenberg, J.E., Samankassou, E., Vennemann, T. and Schaltegger, U., 2019. The driving mechanisms of the carbon cycle perturbations in the late Pliensbachian (Early Jurassic). Scientific Reports, 9, 1-12.

de Wit, M.J., Stankiewicz, J. and Reeves, C., 2008. Restoring Pan-African-Brasiliano connections: more Gondwana control, less Trans-Atlantic corruption. Geological Society, London, Special Publications, 294, 399-412.

de Wit, M., 2007. The Kalahari Epeirogeny and climate change: differentiating cause and effect from core to space. South African Journal of Geology, 110, 367-392.

de Wit, M.J., Linol, B., Furnes, H., Muedi, T. and Valashiya, K., 2020. Pillow talk: Volcanic rocks of the karoo that formed many leagues under the gondwanan sea. South African Journal of Geology, 123, 297-330.

Duncan, R.A., Hooper, P.R., Rehacek, J., Marsh, J.S., and Duncan, A.R., 1997. The timing and duration of the Karoo igneous event, southern Gondwana. Journal of Geophysical Research, 102, 18127-18138.

du Toit, A.L., 1911a. Geologically serveying in 1911-14 by A.L, du Toit, Western Portion of Matatiele in 1902 by Scwarz and Rogers, A.W.

du Toit, A.L., 1911b. Geological survey of part of the Transkei. Sixteenth annual report of the geological commission, 87-136.

du Toit, A.L., 1920. The Karoo dolerite of South Africa: A study in hypabyssal Intrusion. Transaction of the Geological Society of South Africa, 23, 1-42.

du Toit, A.L., 1937. Our Wandering Continents: An Hypothesis of Continental Drifting. Oliver and Boyd; First Edition, 1-368.

du Toit, A.L., 1954. The geology of South Africa. In: B. Haughton and S.H., Olive (Editor) The Karoo system. Edinburgh, 260pp.

Elliot, D.H., Fleming, T.H., Kyle, P.R. and Foland, K.A., 1999. Long-distance transport of magmas in the Jurassic Ferrar Large Igneous Province, Antarctica. Earth and Planetary Science Letters, 167, 89-104.

Elliot, D.H. and Fleming, T.H., 2008. Physical volcanology and geological relationships of the Jurassic Ferrar Large Igneous Province, Antarctica. Journal of Volcanology and Geothermal Research, 172, 20-37.

Encarnación, J., Fleming, T.H., Elliot, D.H. and Eales, H.V., 1996. Synchronous emplacement of Ferrar and Karoo dolerites and the early breakup of Gondwana. Geology, 24, 535-538.

Fildani, A., Weislogel, A., Drinkwater, N.J., McHargue, T., Tankard, A., Wooden, J., Hodgson, D. and Flint, S., 2009. U-Pb zircon ages from the southwestern Karoo Basin, South Africa - Implications for the Permian-Triassic boundary. Geology, 37, 719-722.

Greber, N.D., Davies, J.H.F.L., Gaynor, S.P., Jourdan, F., Bertrand, H. and Schaltegger, U., 2020. New high precision U-Pb ages and Hf isotope data from the Karoo large igneous province; implications for pulsed magmatism and early Toarcian environmental perturbations. Results in Geochemistry, 1, 100005.

Ivanov, A.V., Meffre, S., Thompson, J., Corfu, F., Kamenetsky, V.S., Kamenetsky, M.B. and Demonterova, E.I. 2017., Timing and genesis of the Karoo-Ferrar large igneous province: New high precision U-Pb data for Tasmania confirm short duration of the major magmatic pulse. Chemical Geology, 455, 32-43.

Johnson, M.R., Anhaeusser, C.R. and Thomas, R.J., 2006. The Geology of Southern Africa. In: Sedimentary rocks of the Karoo supergroup.

Jourdan, F., Bertrand, H. and Watkeys, M.K., 2007., From flood basalts to the inception of oceanization: Example from the $^{40}Ar/^{39}Ar$ high-resolution picture of the Karoo large igneous province. Geochemistry, Geophysics, Geosystems, 8, 1-20.

Jourdan, F., Féraud, G., Bertrand, H., Kampunzu, A.B., Tshoso, G., Le Gall, B., Tiercelin, J.J. and Capiez, P., 2004. The Karoo triple junction questioned: Evidence from Jurassic and Proterozoic $^{40}Ar/^{39}Ar$ ages and geochemistry of the giant Okavango dyke swarm (Botswana). Earth and Planetary Science Letters, 222, 989-1006.

Jourdan, F., Féraud, G., Bertrand, H., Kampunzu, A.B., Tshoso, G., Watkeys, M.K., Le Gall, B., 2005. Karoo large igneous province: Brevity, origin, and relation to mass extinction questioned by new $^{40}Ar/^{39}Ar$ age data. Geology, 33, 745-748.

Jourdan, F., Féraud, G., Bertrand, H., Watkeys, M.K. and Renne, P.R., 2007. Distinct brief major events in the Karoo large igneous province clarified by new $^{40}Ar/^{39}Ar$ ages on the Lesotho basalts. Lithos, 98, 195-209.

Kasbohm, J., Schoene, B. and Burgess, S., 2021. Radiometric Constraints on the Timing, Tempo, and Effects of Large Igneous Province Emplacement. In: Large Igneous Province: A driver of Global Environmental and Biotic Changes. Geophysical Monograph 255, 27-82.

Kay, S.M., Ramos, V.A., Mpodozis, C. and Sruoga, P., 1989. Late Paleozoic to Jurassic silicic magmatism at the Gondwana margin: Analogy to the Middle Proterozoic in North America? Geology, 17, 324-328.

Keller, C.B., Schoene, B. and Samperton, K.M., 2018. A stochastic sampling approach to zircon eruption age interpretation. Geochemical Perspectives Letters, 8, 31-35.

Kinney, S.T., MacLennan, S.A., Keller, C.B., Schoene, B., Setera, J.B., VanTongeren, J.A. and Olsen, P.E., 2021. Zircon U-Pb Geochronology Constrains Continental Expression of Great Meteor Hotspot Magmatism. Geophysical Research Letters, 48, e2020GL091390.

Kleiman, L.E. and Japas, M.S., 2009. The Choiyoi volcanic province at 34°S-36°S (San Rafael, Mendoza, Argentina): Implications for the Late Palaeozoic evolution of the southwestern margin of Gondwana. Tectonophysics, 473, 283-299.

Krogh, T.E., 1973. A low-contamination method for hydrothermal decomposition of zircon and extraction of U and Pb for isotopic age determinations. Geochimica et Cosmochimica Acta, 73, 485-494.

Linol, B., de Wit, M.J., Milani M.J., Guillocheau, F. and Scherer, C., 2015. New regional correlations between Congo, Parana and Cape-Karoo Basins of the Southwest Gondwana. In: M. de Wit (Editor), Geology and Resource Potential of the Congo Basin, Regional Geology Reviews. Springer-Verlag Berlin Heidelberg 2015, 245-268.

Lock, B.E., Paverd, A.L. and Broderick, T.J., 1970. Stratigraphy of the karroo volcanic rocks of the barkly east district. Transactions of the Geological Society of South Africa, 77, 117-129.

Lock, B.E., Paverd, A.L., Lock, B.E., Paverd, A.L. and Broderick, T.J., 1974. Stratigraphy of the Karroo volcanic rocks in the Barkly East District. South African Journal of Geology, 77, 117-129.

López-Gamundí, O., 2006. Permian plate margin volcanism and tuffs in adjacent basins of west Gondwana: Age constraints and common characteristics. Journal of South American Earth Sciences, 22, 227-238.

McLean, N.M., Condon, D.J., Schoene, B. and Bowring, S.A., 2015. Evaluating uncertainties in the calibration of isotopic reference materials and multi-element isotopic tracers (EARTHTIME Tracer Calibration Part II). Geochimica et Cosmochimica Acta, 164, 481-501.

Moore, A., 1965. The North Gap Dyke of the Transkei. Transaction and Proceedings of the Geological Society of South Africa, 68, 89-119.

Morake, M.A., O'Kennedy, J.N.F., Knoper, M.W., de Kock, M., Kramers, J.D., Grantham, G.H., Belyanin, G. and Elburg, M.A., 2021. The age and palaeomagnetism of Jurassic dykes, western Dronning Maud Land: implications for Gondwana breakup. Geological Society, London, Special Publications, SP518-2021-44.

Moulin, M., Fluteau, F., Courtillot, V., Marsh, J., Delpech, G., Quidelleur, X., Gérard, M. and Jay, A.E., 2011. An attempt to constrain the age, duration, and eruptive history of the Karoo flood basalt: Naude's Nek section (South Africa). Journal of Geophysical Research: Solid Earth, 116, 1-27.

Muedi, T.T., 2019. Early Jurassic dolerites of the Karoo Large Igneous Province

(KLIP): an analysis of their age and emplacement history from sea level to the Drakensberg Mountains in the Eastern Cape, South Africa. Nelson Mandela University, 1-291pp.

Mueller, O. and Jokat, W., 2019. Tectonophysics The initial Gondwana break-up: A synthesis based on new potential field data of the Africa-Antarctica Corridor. Tectonophysics, 750, 301-328.

Munizaga, F., Maksaev, V., Fanning, C.M., Giglio, S., Yaxley, G. and Tassinari, C.C.G., 2008., Late Paleozoic-Early Triassic magmatism on the western margin of Gondwana: Collahuasi area, Northern Chile. Gondwana Research, 13, 407-427.

Neumann, E.R., Marsh, J.S., Galerne, C.Y., Polteau, S., Svensen, H. and Planke, S., 2020., Co-existing low-ti and high-ti dolerites in two large dykes in the gap dyke swarm, southeastern karoo basin (South Africa). South African Journal of Geology, 123, 19-34.

Pálfy, J. and Smith, P.L., 2000. Synchrony between Early Jurassic extinction, oceanic anoxic event, and the Karoo-Ferrar flood basalt volcanism. Geology, 28, 747-750.

Pankhurst, R.J., Leat, P.T., Sruoga, P., Rapela, C.W., Márquez, M., Storey, B.C. and Riley, T.R., 1998. The Chon Aike province of Patagonia and related rocks in West Antarctica: a silicic large igneous province. Journal of Volcanology and Geothermal Research, 81, 113-136.

Park, Y., Swanson-Hysell, N.L., Lisiecki, L.E. and Macdonald, F.A., 2020. Evaluating the Relationship Between the Area and Latitude of Large Igneous Provinces and Earth's Long-Term Climate State. In: A.B. Richard, E. Ernst and Alexander J. Dickson (Editor), Large igneous provinces: A Driver of Global Environmental and Biotic Changes. 153-168.

Paton, C., Hellstrom, J., Paul, B., Woodhead, J. and Hergt, J., 2011. Iolite: Freeware for the visualisation and processing of mass spectrometric data. Journal of Analytical Atomic Spectrometry, 26, 2508-2518.

Peace, A.L., Phethean, J.J.J., Franke, D., Foulger, G R., Schiffer, C., Welford, J.K., Mchone, G., Rocchi, S., Schnabel, M. and Doré, A G., 2019. Earth-Science Reviews A review of Pangaea dispersal and Large Igneous Provinces – In search of a causative mechanism. Earth-Science Reviews, 196, 1-25.

Ramezani, J., Hoke, G.D., Fastovsky, D.E., Bowring, S.A., Therrien, F., Dworkin, S.I., Atchley, S.C. and Nordt, L.C., 2011., High-precision U-Pb zircon geochronology of the late triassic chinle formation, Petrififed Forest National Park (Arizona, USA): Temporal constraints on the early evolution of dinosaurs. Bulletin of the Geological Society of America, 123, 2142-2159.

Renne, P.R., Glen, J.M., Milner, S.C. and Duncan, A.R., 1996. Age of Etendeka flood volcanism and associated intrusions in southwestern Africa. Geological society of America, 24, 659-662 (a).

Riley, T.R., Leat, P.T., Curtis, M.L., Millar, I.L., Duncan, R.A. and Fazel, A., 2005. Early-middle Jurassic dolerite dykes from western Dronning Maud Land (Antarctica): Identifying mantle sources in the Karoo large igneous province. Journal of Petrology, 46, 1489-1524.

Ruhl, M., Hesselbo, S.P., Hinnov, L., Jenkyns, H.C., Xu, W., Riding, J.B., Storm, M., Minisini, D., Ullmann, C.V. and Leng, M.J., 2016. Astronomical constraints on the duration of the Early Jurassic Pliensbachian Stage and global climatic fluctuations. Earth and Planetary Science Letters, 455, 149-165.

Schoene, B., Eddy, M.P., Samperton, K.M., Keller, C.B., Keller, G., Adatte, T. and Khadri, S.F.R., 2019. U-Pb constraints on pulsed eruption of the Deccan Traps across the end-Cretaceous mass extinction. Science, 363, 862-866.

Sell, B., Ovtcharova, M., Guex, J., Bartolini, A., Jourdan, F., Spangenberg, J.E., Vicente, J.-C. and Schaltegger, U., 2014. Evaluating the temporal link between the Karoo LIP and climatic–biologic events of the Toarcian Stage with high-precision U-Pb geochronology. Earth and Planetary Science Letters, 408, 48-56.

Sensarma, S., Storey, B.C. and Malviya, V.P., 2018. Gondwana Large Igneous Provinces (LIPs): Distribution, diversity and significance. Geological Society Special Publication, 463, 1-16.

Storey, C.B., 1995. The role of mantle plumes in continental break-up: case histories from Gondwanaland. Nature, 377, 301-308.

Svensen, H., Corfu, F., Polteau, S., Hammer, Ø. and Planke, S., 2012. Rapid magma emplacement in the Karoo Large Igneous Province. Earth and Planetary Science Letters, 325-326, 1-9.

Svensen, H.H., Torsvik, T.H., Callegaro, S., Augland, L., Heimdal, T.H., Jerram, D.A., Planke, S. and Pereira, E., 2017. Gondwana Large Igneous Provinces: plate reconstructions, volcanic basins and sill volumes. Geological Society, London, Special Publications, 463, 17-40.

Viglietti, P.A., Frei, D., Rubidge, B.S. and Smith, R.M.H., 2018. U-Pb detrital zircon dates and provenance data from the Beaufort Group (Karoo Supergroup) reflect sedimentary recycling and air-fall tuff deposition in the Permo-Triassic Karoo foreland basin. Journal of African Earth Sciences, 143, 59-66.

Walker, F., 1943. The origin of the Kentani gap dyke of the Transkei, Cape Province. Royal Society of South Africa, Transaction, 30, 79-83.

Editorial handling: M.A. Elburg.